



# CHARACTERIZATION OF RAW ZEOLITE AND SURFACTANT-MODIFIED ZEOLITE AND THEIR USE IN REMOVAL OF SELECTED ORGANIC POLLUTANTS FROM WATER

MAHA M. HUSSEIN<sup>a</sup>, KHALIL M. KHADER<sup>a</sup> and SALEM M. MUSLEH\*

Chemistry Department, Faculty of Science, Al-Balqa Applied University, AL-SALT, 19117, JORDAN

<sup>a</sup>Department of Earth and Environmental Sciences, Faculty of Science, Hashemite University, ZARQA, 13115, JORDAN

## ABSTRACT

Increases in environmental pollutants led to use of natural low cost materials such as zeolite, which prove their effective in water treatment. Natural zeolite obtained from Jabal Hannoun (local) and imported zeolites, clinoptilolite-rich tuff obtained from U.S.A, Syrian zeolitic tuff, and synthetic faujasite-13X were used as adsorbent. Characterization of raw and modified zeolite has been studied to verify their physical chemical and mineralogical properties, in order to note any changes occur during the modification of zeolite. The feasibility of using surfactant-modified zeolite to remove aniline and its derivatives from water in the broad band of concentrations (5-200 mg L<sup>-1</sup>) was evaluated by batch experiments. The results showed that a significant increase in aniline and its derivatives sorption capacity could be achieved at the loading level of hexadecyltrimethylammonium, a cationic surfactant, on zeolite surfaces at monolayer coverage. Adsorption equilibrium was carried out at different initial concentrations and different pH varies from 3 to 11. Langmuir and Freundlich adsorption isotherms were applied to the experimental data. The data best fitted the Freundlich model. It was found that the aniline removal efficiency by using clinoptilolite-rich tuff has the highest maximum adsorption 50% compared to the other zeolite. The maximum efficiency removal for N-Methylaniline reached upto 69.5% by using Syrian-zeolite. A decrease in N,N-Dimethylaniline removal by surfactant-modified zeolite, and the maximum efficiency removal was 16% by using Jordanian-Faujasite.

The results show that the optimum pH of the adsorption of aniline and its derivatives by surfactant-modified zeolite was almost in acidic and neutral pH conditions. Characterization of raw and surfactant-modified zeolite was carried out using several techniques such as cation exchange capacity, X-ray diffraction, X-ray fluorescence, scanning electron microscopy, and Fourier Transform Infrared Spectroscopy. UV/VIS spectrophotometer was used in equilibrium analysis.

**Key words:** Surfactant, Modification, Pollutants, Zeolite.

---

\* Author for correspondence; E-mail: [smusleh@lycos.com](mailto:smusleh@lycos.com)

## INTRODUCTION

Protection of the natural water resources from contamination with toxic organic and inorganic materials requires development of efficient method for purification of industrial and domestic wastewater<sup>1</sup>.

Industrial wastewater is considered as a major environmental problem. Many researches and studies have been applied to treat and solve the environmental problems resulted from the industry to remove the pollutants. One branch of these is water purification by using surfactant-modified zeolites to remove the toxic organic compounds<sup>2</sup>. The surfactants like hexadecyltrimethylammonium (HDTMA) increase the surface area of the zeolite and accordingly increase the ability of the adsorption<sup>3</sup>. The unique structure of zeolites gives rise to remarkable physical and chemical properties, such as ion exchange, reversible dehydration, adsorption, and molecular sieve, which have allowed the group to play a vital role in many industrial and agricultural technologies<sup>4</sup>. Water pollution occurs when water is adversely affected due to the addition of large amount of materials to the water<sup>5</sup>. Jordan is one country facing continuous water pollution problems; reports indicated that the water resources have a high level of toxicity<sup>6,7</sup>.

This work deals with characterization of different types of zeolite (natural and synthetic zeolites), comparison between them, modification of zeolite using cationic surfactant (Hexadecyltrimethylammonium-Br), characterization of modified-surfactant zeolite (SMZ) and study the efficiency to remove organic pollutant by SMZ from water, the selected organic pollutant was aniline and its derivatives.

## EXPERIMENTAL

### Methods and materials

#### Characterization of natural and synthetic zeolites

#### Petrography and mineralogical study

A mixture of epoxy-hardener was prepared by using a ratio 5:1 in suitable container, used to cover different types of zeolite samples. Then left for one hour in the container evacuation pump until the impregnation was completed. The samples were left overnight to become hard and ready for grinding and prepared using conventional thin section techniques.

### **Cation Exchange Capacity (CEC)**

The method adopted in this study is the Modified-Kjeldahl Method without Digestion<sup>8</sup>. The solid samples were added to a 800 mL Kjeldahl flask and then mixed with 25 mL of 0.1 N NaOH, and distilled 50 mL of 2% H<sub>3</sub>BO<sub>3</sub>. Ten drops of bromocresol green methyl red mixed indicator were added and stirred rapidly. The boric acid solution was titrated with standard 0.1 N H<sub>2</sub>SO<sub>4</sub>, at the end point the color was changed from bluish-green to pink.

Cation exchange capacity experiment was made twice and the average was calculated, according to the following equation:

$$\text{CEC meq/100 g} = A \times N / \text{g (sample)},$$

where: A = volume of H<sub>2</sub>SO<sub>4</sub> used for sample in mL, N = Normality of NaOH

### **Water adsorption capacity**

To determine the hydration dehydration characteristics for natural and synthetic zeolite, one gram of each zeolite types were combusted under different temperatures (100, 200, 300, 400, 500, and 600°C) for 2 hrs then left to cool in a desiccator for 15 min. Periodically the weight of sample was measured, and then left at room temperature and reweigh every 2 hrs until a constant weight was achieved.

### **Chemical analysis**

Dry natural and synthetic zeolite samples were crushed by milling machine for 1-5 min to fine powder. 8.0 g of the powder samples and 2 g of binder wax were homogenized by mixing, pressed in small aluminum cup under pressure of about 200 KN for 30 seconds to get a disc of the sample with 40 mm diameter and 4 mm thickness. The XRF instrument Philips Magix PW-2424 operated at 50 KV and 10 mA was used to analyze the major oxides in these samples.

### **Surface area measurements**

Surface area experiment was carried out using methylene blue pigment. Different weight of natural zeolites ranges from (0.02-0.2 g) was added to 100 mL screw cap flasks, each one contain 50 mL of 200 mg/L of methylene blue. Samples were shaken in a thermostatic shaker at 150 rpm and at temperature 25°C for three days to reach equilibrium. The samples were filtered and diluted to a certain concentration, and the supernatant was analyze using UV/VIS spectrophotometer at wavelength 664 nm using a calibration curve of standard methylene blue solutions as seen in Fig. 1.

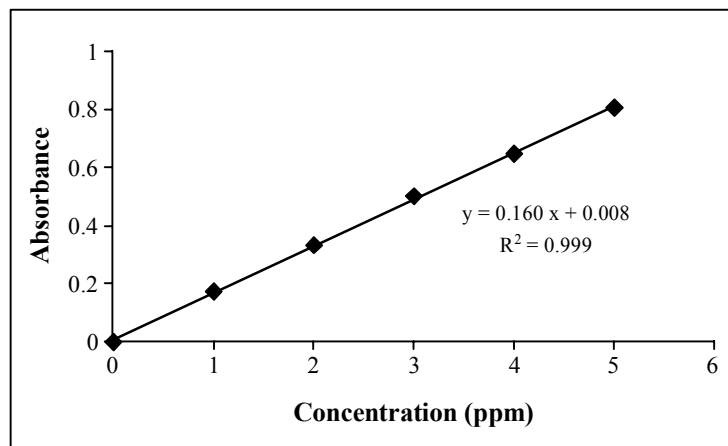


**Fig. 1: Calibration curve of standard methylene blue solutions**

### **pH measurement**

The pH of natural and synthetic zeolite was measured by mixing 0.1 g of the different zeolite types with 10 mL of distilled water and shaken for 24 h at 30°C. The samples were then filtered, and the pH of the solution was determined using a pH-meter.

### **Modification of zeolite samples by cationic surfactant (HDTMA-Br)**

Natural zeolite (Jordanian-Faujasite, Syrian, and Clinoptilolite-rich tuff) and synthetic faujasite-13X was modified by HDTMA-Br at 100% and 200% of ECEC. 100% represent monolayer coverage and 200% represent bilayer coverage<sup>9</sup>.

About 30 g of raw zeolites were mixed with 90 mL of 50 and 67 mmol/L of HDTMA-Br to obtain 100% and 200% of its ECEC, respectively. Zeolite mixture was shaken for 8 hr at 25°C and 150 rpm on a thermostatic shaker, followed by centrifuging and washing with two portions of distilled water. The surfactant-modified samples were then air dried prior to further use, showed that final HDTMA surface coverage for surfactant-modified zeolite prepared in this manner were 98-100% of the target values<sup>10</sup>.

### **Analytical measurements**

The prepared concentration of aniline and its derivative in this study range between 5-200 mg/L (ppm). Absorbance measurements were done by UV/VIS spectrophotometer, the maximum absorbance ( $\lambda_{\max}$ ) of aniline and its derivative were determined by scanning a standard solution of known concentration at different wavelength. Values of maximum absorbance were recorded and the ( $\lambda_{\max}$ ) of aniline, N-Methylaniline and N,N-Dimethylaniline

was 254, 270, and 280 nm, respectively. These wavelengths were used for preparation of calibration curves shown in Fig. 2.

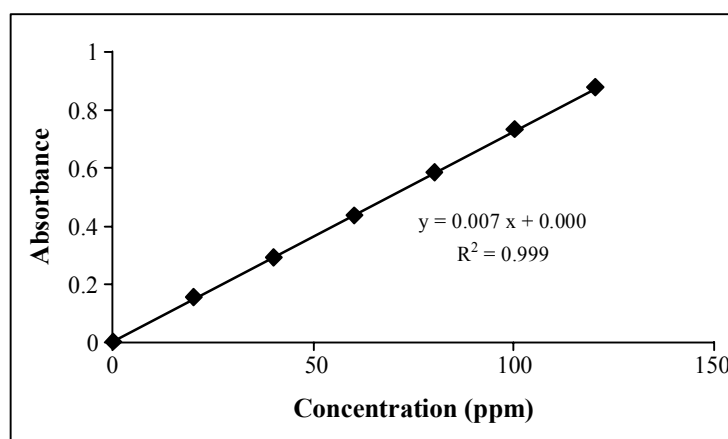


**Fig. 2: Calibration curve of standard aniline solutions**

### **Batch method**

All adsorption experiments in this work were performed by batch technique. Aniline and N-Methylaniline were prepared in distilled water, N,N-Dimethylaniline was dissolved in ethanol as organic solvent. The adsorption process was affected by several parameters; the initial concentration and pH were studied.

### **Chemical constitutions**

The FTIR spectra in the range of 400-4000  $\text{cm}^{-1}$  were recorded using a Magna-IR 560 E.S.P spectrometer equipped with (OMNIC) software. The samples were prepared by the standard KBr method. A very small amount of the solid (approximately 1-2 mg) is added to pure potassium bromide powder (approximately 200 mg) and ground up as fine as possible. Then placed in a small disk and subjected pressure mechanically. The pressure is maintained for several minutes before removing the disk and the KBr disk formed. The disk is then placed in a sample holder ready for scanning.

## **RESULTS AND DISCUSSION**

### **Characterization of unmodified zeolites samples**

#### **Sample preparation**

Jordanian-Faujasite was crushed and sieved to different particle size ranges between

(2.36-0.0425 mm). The mass of each fraction size and the mass percentage are shown in Table 1.

**Table 1: Particle size, mass, and mass percentage**

Particle size (mm)	Mass (g)	Mass %
2.36-2.0	470.21	24.14
2.0-1.0	243.57	12.51
1.0- 0.30	358.27	18.40
0.30-0.0425	203.35	10.44
Pan	657.71	33.77
Total	1933.11	99.26

The fraction size that contains highest zeolite content is the size in range between 1.0-0.3 mm<sup>11</sup>. Other beneficiation of diagenetic zeolites from the volcanic tuff of NE-Jordan has revealed that zeolites are concentrated in the (0.5-0.25) mm and (0.25-0.125) mm size fractions<sup>12</sup>. All experiments in this work were within the range of 1.0-0.3 mm. The relationship between particle size and mass (%) are portrayed in Fig. 3.

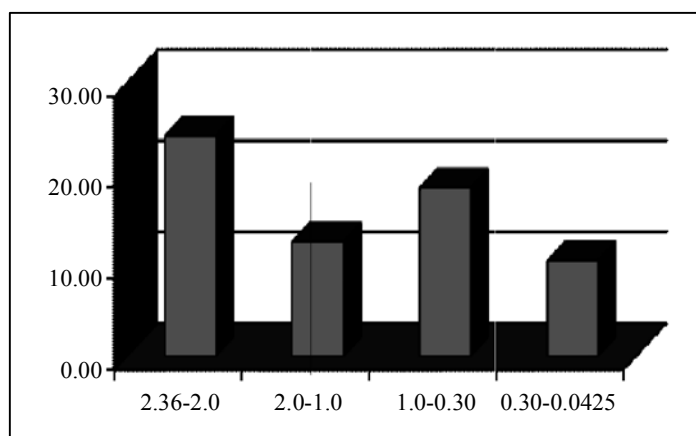


**Fig. 3: Relationship between particle size and mass (%) of raw Jordanian-Faujasite**

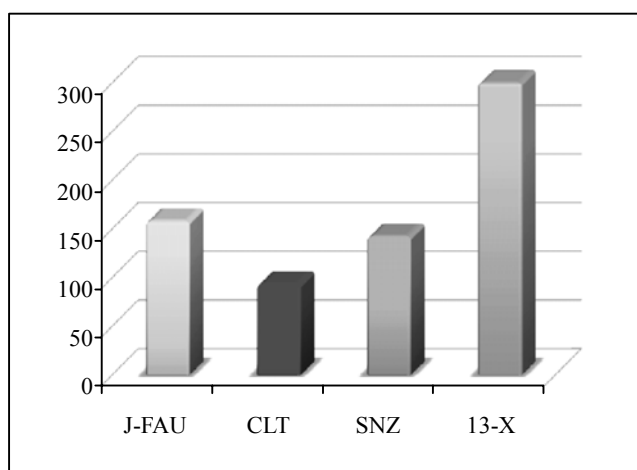
### Cation exchange capacity

The cation exchange capacity of the four types of zeolite samples varies between 90 to 301 meq/100 g. CEC values for the different type of zeolite were calculated in Table 2, which represents the average of two trials.

**Table 2: CEC of the different types of zeolite**

Zeolite type	CEC (meq/100 g)
Jordanian-Faujasite	158
Clinoptilolite-rich tuff	93
Syrian-natural zeolite	142
Synthetic faujasite-13X	300

The highest cation exchange capacity was found in synthetic faujasite-13X, followed by Jordanian zeolite, Syrian zeolite, and the last one was Clinoptilolite-rich tuff, as seen in Fig. 4.

**Fig. 4: Average CEC for the different types of zeolite**

These results can be simply explained according to the selectivity of the exchangeable cations, which depends mainly on the polarity and the diffusing cations<sup>4</sup>, as shown in Table 3.

**Table 3: Radius of the different cations**

Cations	NH <sub>4</sub> <sup>+</sup>	Ca <sup>+2</sup>	K <sup>+</sup>	Mg <sup>+2</sup>	Na <sup>+</sup>
Radius (Å)	1.47	0.99	1.38	0.72	1.02

As shown in the table above, the highest selectivity of NH<sub>4</sub><sup>+</sup> ion (1.47 Å) is toward K<sup>+</sup> ion (1.38 Å) and Na<sup>+</sup> (1.02 Å) due to the similarity in radius and charge. This substitution

of  $K^+$  ion and  $Na^+$  by  $NH_4^+$  ion explains the high CEC value for synthetic zeolite (13-X) depend upon theoretical formula.

The cation exchange capacity of Clinoptilolite variations depend on the location of the deposits<sup>13</sup>. The CEC of Clinoptilolite from St. Cloud mining company ranges between 0.8 to 1.2 meq/g, (80 to 120 meq/100 g).

### pH measurements

Zeolite is considered as alkali and alkaline earth metal elements and the results of pH-experiment shows that all different types of zeolite are alkaline. This is due to the reaction of zeolite with distilled water as a result of cation exchange, ( $Na^+$ ,  $K^+$  with  $H^+$ ), and the excess quantity of  $OH^-$  is remaining in the solution. Table 5 shows the pH values got from the experiments. The highest pH value is 10.05 for synthetic faujasite-13X, and the lowest is 7.54 for clinoptilolite-rich tuff zeolite.

**Table 4: pH values of the different types of zeolite**

Zeolite type	J-FAU	CLT	SNZ	13-X
Average	7.77	7.54	9.86	10.05

### Specific gravity

As shown in Table 6 below, the average value of specific gravity for the different types of zeolite ranges from 2.13 to 2.31  $g/m^3$ , which is with agreement of about 1.90 to 2.27  $g/m^3$  according to Breck and Deer<sup>4,14</sup>. The results of the specific gravity experiment show that the highest reading is 2.33  $g/m^3$  which represent the Syrian zeolite type while the lowest reading is 2.12  $g/m^3$ , which represent Jordanian-Faujasite. The synthetic faujasite-13X is powder; there was no true comparison with the other zeolite specific gravities.

**Table 5: Specific gravity of different type zeolites**

Zeolite type	J-FAU	CLT	SNZ
Specific gravity ( $g/m^3$ )	2.13	2.16	2.31

### Effect of temperature on water content

**Dehydration:** Dehydration property of the natural (local and imported) and synthetic zeolite was examined under different temperature ranges from 100-600°C. As illustrated in Fig. 5. Dehydration varies within this temperature range from 7.06% to 21%.



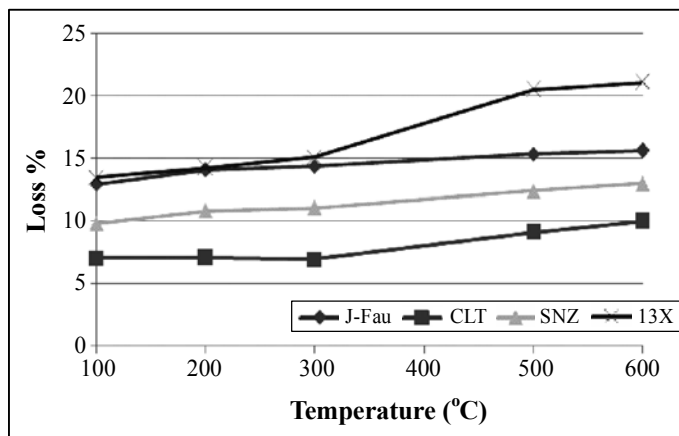


**Fig. 5: Dehydration curves of the different zeolite types at different temperature**

The dehydration curves for the different types of zeolite shown in Figure 5 indicate a maximum water loss is found in synthetic faujasite 13X, which is about 21% occurring closed to 600°C. The relationship between temperature and the loss % is proportional for all types of zeolite. The maximum water loss is 15.6% and 13% occurred at 600°C for Jordanian and Syrian zeolite, respectively. Furthermore, Clinoptilolite-rich tuff has a maximum water loss of about 10% occur at 600°C.

### Water absorption capacity

The capacity of the different types of zeolite to regain water was examined under different temperature ranges from 100°C to 600°C. The results show a maximum percentage of water absorption capacity of 24.38% for the synthetic faujasite 13X at 500°C.

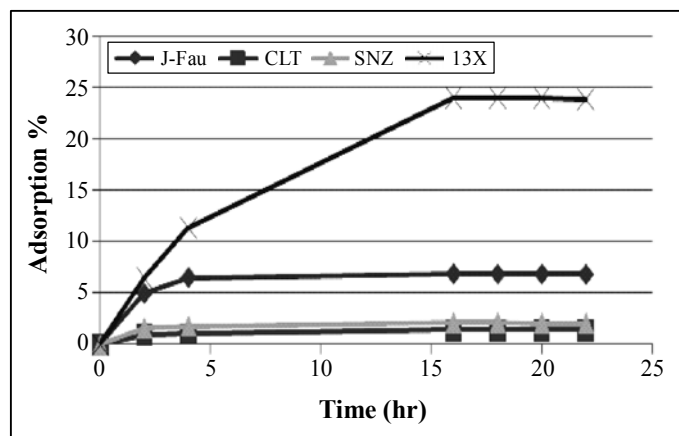


**Fig. 6: Water absorption capacity of the different zeolite types at 600°C**

While the maximum percentages of water absorption capacity of the other zeolite types are 12.65%, 6.43%, 5.39% for the Jordanian-Faujasite, Syrian-zeolite, and Clinoptilolite-rich tuff, respectively occurring at 300°C. All natural zeolites as indicated in Fig. 6 exhibit decreasing in the water absorption capacity with increasing the temperature above 300°C due to the thermal instability of the zeolite structure<sup>15</sup>.

### **Minerals identification**

The identification of the different zeolite types were carried out using the XRD technique. With respect to Jordanian zeolite different peaks describe different mineral, the main zeolite minerals in the original sample are faujasite (FAU) at many angles 6.2°, 23.6°, 31.3°, and 39.8°, Phillipsite (PHI) has many peaks at different angles 12.5°, 15.6°, and 28°. There is some other non-zeolite minerals include calcite (Cc) at angle 29.5°. XRD analysis for Clinoptilolite-rich tuff indicated high presence of clinoptilolite (CLT) mineral at angles 9.8°, 11.1°, 22.4°, and 26.6°, calcite mineral has been also indicated at angle 29.9° as non-zeolitic mineral. For Syrian zeolite the XRD analysis demonstrates one distinguished peak which represents a large amount of calcite (Cc) at angle 29.4°, also phillipsite mineral appears at different angles as a zeolite mineral besides to Montmorillonite (clay mineral). Finally synthetic faujasite-13X all peaks describes the faujasite mineral at different angles as seen in Fig. 14.

### **Chemical compositions**

The chemical compositions of the different zeolite types using XRF and considered as major oxides are SiO<sub>2</sub>, Al<sub>2</sub>O<sub>3</sub>, MgO, CaO, K<sub>2</sub>O, Na<sub>2</sub>O, which is incorporated within the zeolite structure. Other oxides, such as Fe<sub>2</sub>O<sub>3</sub>, TiO<sub>2</sub>, P<sub>2</sub>O<sub>5</sub>, and MnO, correspond to the presence of non-zeolite accessory phase. The high content of CaO in the Jordanian-Faujasite and Syrian natural zeolite is attributed to the presence of calcite. There is a variation in the major oxide percentage as a result of differences in zeolite types (local and imported zeolites). These differences are due to the original material and depositional environments that formed the zeolitic tuff deposits.

### **Scanning Electron Microscope (SEM)**

All samples have been studied under scanning electron microscopes (SEM), to recognize the morphology of the zeolite minerals surface.

### **Jordanian zeolites**

#### **(a). Faujasite**

According to Ibrahim<sup>11</sup>, faujasite occur as isotropic rim enclosing palagonite clasts

and preceding the crystallization of phillipsite. SEM image shows the part of faujasite preceding the crystallization of phillipsite Fig. 7.

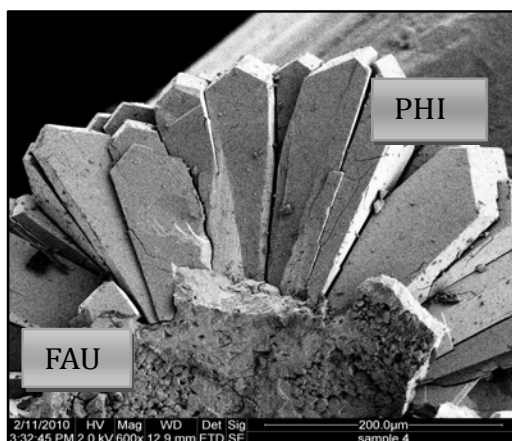


**Fig. 7:** SEM shows a part of faujasite and radiating phillipsite

### **(b). Phillipsite**

Phillipsite is the most abundant zeolite mineral that appears under SEM. Phillipsite occur as radiating crystal as seen previously in Fig. 7. Phillipsite also occur as prismatic crystals as shown 8.

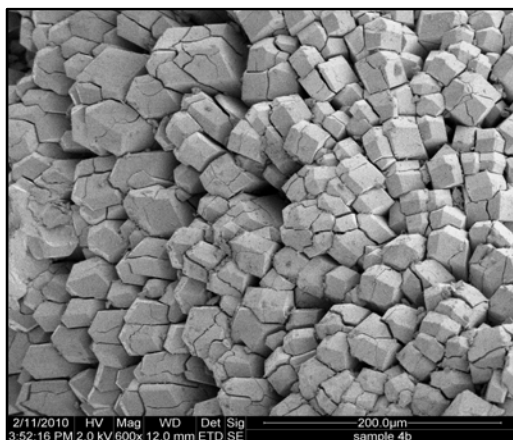


**Fig. 8:** SEM shows prismatic phillipsite crystal

### Clinoptilolite-rich tuff

Clinoptilolite mineral was investigated as thin bladed crystals; Fig. 9 shows a group of clinoptilolite crystals.

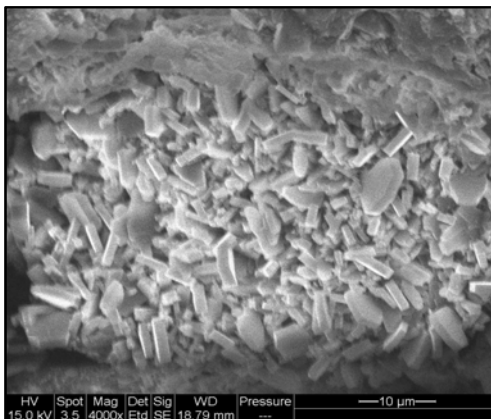


**Fig. 9: SEM shows thin bladed clinoptilolite crystals**

### Synthetic Faujasite-13X

Synthetic faujasite appears under electron microscope as spheroidal aggregate of cubic crystal as shown in Fig. 10.

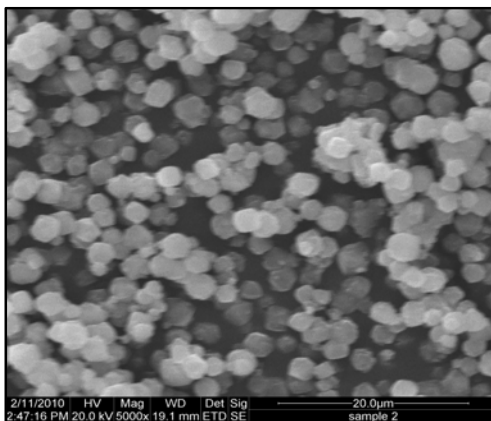


**Fig. 10: SEM shows spheroidal cubic synthetic faujas**

Jordanian-Faujasite, Syrian zeolite, and Clinoptilolite-rich tuff have been studied under polarizing microscope to identify the zeolitic tuff composition and textural relationship.

Jordanian-Faujasite tuff composed primary of angular to sub-angular vesicular lapilli clasts made of palagonitized volcanic glass as brown to black color and iron oxides. Calcite occurs as coarse-grained rim preceding phillipsite mineral (Plate 1B). Rock fragment from the basalt was recorded; Olivine occurs as euhedral crystal distinguished usually by fracture and pale-yellow to green color. Phillipsite (Ph) occurs mainly as white, radiating crystal aggregates forming a thin rim on the granules or inside vesicles (Plate 1A), phillipsite also occur as rosettes of radiating crystal. Faujasite (Fa) occur as continuous or discontinuous isotropic rim (Plates 1B) usually not uniform in thickness, enclosing palagonite clasts and preceding the crystallization of phillipsite. Chabazite (Ch) also recorded, as rhombohedra, and occur as colorless transparent crystals.

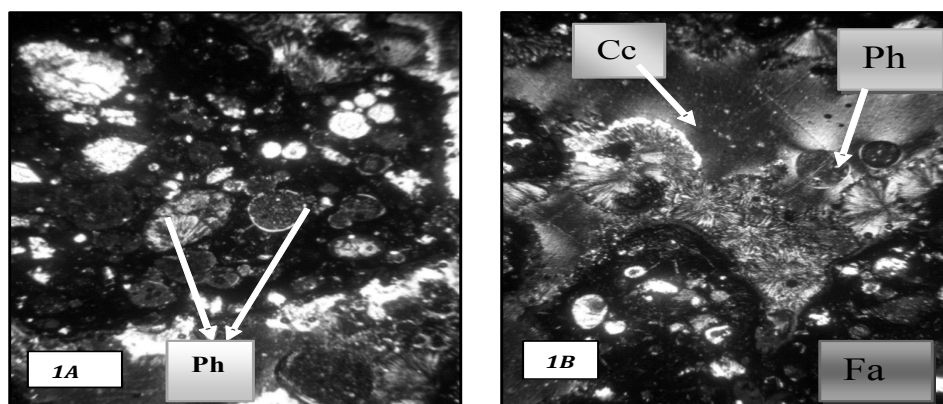


**Fig. 11: Photomicrograph of Jordanian zeolites**

Clinoptilolite-replaced glass in the calcite-cemented tuff. Crystals of mainly clinoptilolite as needle like-shape. Syrian zeolite the most abundant minerals is Clinopyroxene (Augite) wish occur as prismatic crystals distinguished by imperfect cleavage, with pleochriysim. Phillipsite mineral found in the sample as fibrous or radiated crystals. Rock fragments, crystals are welded together by ash material; most of it is pyroclastic.

### **Chemical constitutions and IR interpretation**

The infrared method has been demonstrated to be useful for determining zeolite framework structures and compositions in studies on synthetic<sup>16,17</sup> and natural samples<sup>18,19</sup>. In the FTIR spectra of zeolite samples four groups of bands are present: The bands due to the presence of zeolite water ranges between 1600-3700  $\text{cm}^{-1}$ . The bands connected with the internal Si-O (Si) and Si-O (Al) vibrations in tetrahedral or alumino- and silico-oxygen bridges are in the range of 400-1200  $\text{cm}^{-1}$ . The bands due to the pseudo-lattice vibrations of

structural units ranges of 500-700  $\text{cm}^{-1}$ . The bands due to T-O bending are of 400-500  $\text{cm}^{-1}$ . A broad band in the range of 3300-3700  $\text{cm}^{-1}$  and another broad band in the range of 980-1230  $\text{cm}^{-1}$ , are due to the stretching vibrations of Si (Al)-O, this band is sensitive to the content of Al and Si. At peak of 1650  $\text{cm}^{-1}$  this is due to H-O-H bending<sup>20,21</sup>. The IR absorption spectra of the un-modified zeolite samples were measured, peaks analysis obtained from the spectra are shown in Table 6.

**Table 6: Infrared absorption bands of Un-Modified zeolite samples**

Jordanian Zeolite	Syrian Zeolite	Clinoptilolite-rich tuff	Synthetic Faujasite-13X	Assignment
421.37	449.21	461.72	462.70	[T-O] at 400-500 $\text{cm}^{-1}$
1024.00	1020.25	1049.26	1015.84	[Si-O-Si(Al) at 1000-1200 $\text{cm}^{-1}$
1654-3672	1645-3444	1644-3671	1642-3472	[H <sub>2</sub> O] at 1600-3700 $\text{cm}^{-1}$

### Surface area

To estimate the surface area only for Jordanian-Faujasite and Syrian natural zeolite, methylene blue method was applied. Linearized Langmuir adsorption isotherm ( $C_e$  vs.  $C_e/Q_e$ ) was used to determine the  $Q_m$  (Maximum adsorption capacity), Figs. 12 and 13.

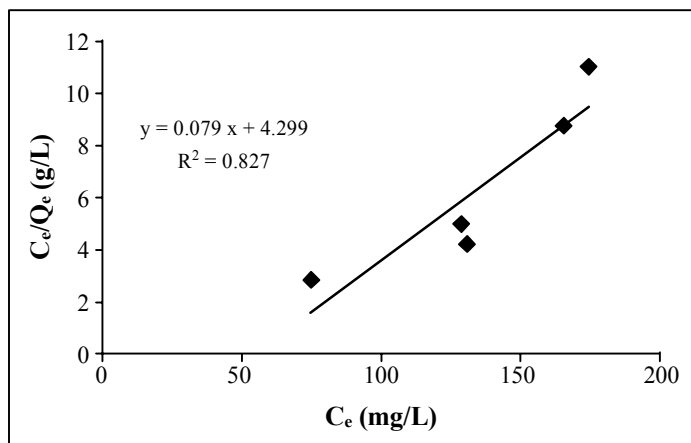


**Fig. 12: Linearized langmuir adsorption isotherm of Jordanian-Faujasite**

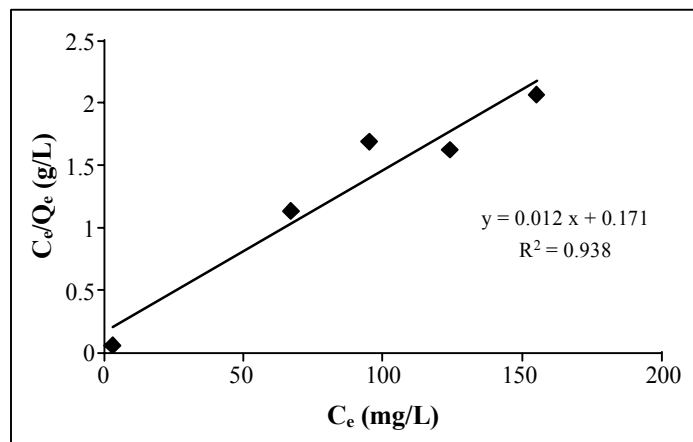


**Fig. 13: Linearized Langmuir adsorption isotherm of Syrian zeolite**

Maximum adsorption capacity was 14 mg/g and 83 mg/g for Jordanian-Faujasite and Syrian zeolite, respectively. To calculate the surface area equation below was used:

$$S = Q_m \cdot N \cdot A_m \times 10^{-20}$$

From this equation, surface area was calculated as 36.1 (m<sup>2</sup>/g) and 214.79 (m<sup>2</sup>/g) for Jordanian-Faujasite and Syrian zeolite. This result gives an indication of the ability of zeolite to adsorb Methylene blue; Syrian zeolite has the higher ability to adsorb methylene blue more than Jordanian-Faujasite.

### **Characterization of surfactant-modified zeolite**

Zeolite samples were modified using HDTMA-Br as surfactant and the modification was at 100% (monolayer coverage). Samples were characterized by –

#### **Anion Exchange Capacity (AEC)**

Hence, the natural zeolites can exchange cations the cationic surfactants have a great affinity to this negative charge. This property has been used to modify the external surface of the zeolites by adsorbing a cationic surfactant to improve its anion exchange capacity<sup>23</sup>.

Anion exchange capacity for the surfactant-modified zeolites was determined; following the same procedure that applied for the raw zeolite (Kjeldahl method). The results of the experiment are shown in Table 7.

**Table 7: AEC of Surfactant-Modified Zeolite**

Zeolite type	AEC (meq/100 g)
Jordanian-Faujasite	121
Clinoptilolite-rich tuff	69
Syrian natural zeolite	110
Synthetic Faujasite-13X	270

As a comparison to the CEC of raw zeolite (158, 93, 142, and 300 meq/g) for Jordanian-Faujasite, Clinoptilolite-rich tuff, Syrian zeolite, and Synthetic faujasite-13X, respectively, the anion exchange capacity for the modified zeolites were less than the CEC, this is due to the fact that the surfactant decrease the surface area and the pore volume as a result of obstructed some of the main channels of the zeolite<sup>24</sup>.

### Mineral identification

XRD analysis was applied to surfactant-modified zeolite samples to clarify any changes occur as a result of samples modification. The results are shown in Figs. (14, 15). The results are compared to un-modified zeolite samples.

A part from differences from the intensity of the XRD peak there are no changes in zeolite mineral, as noticed from the figures, and this is in agreement with literature<sup>25</sup>.

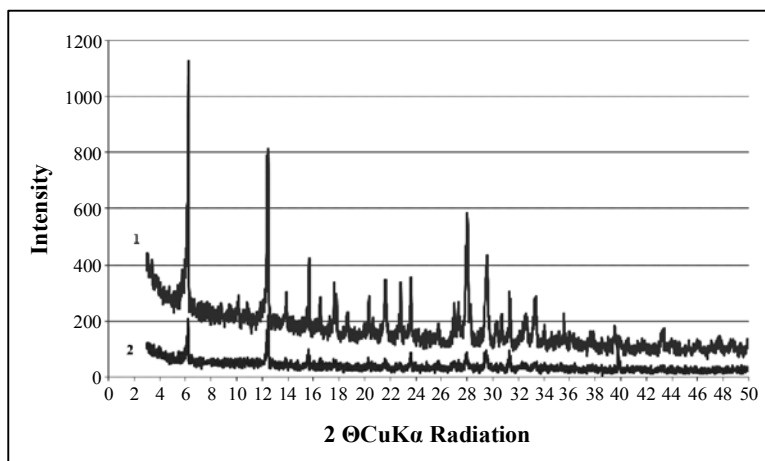


**Fig. 14: XRD diffractogram of modified Jordanian-Faujasite (1) compared to raw Jordanian-Faujasite (2)**



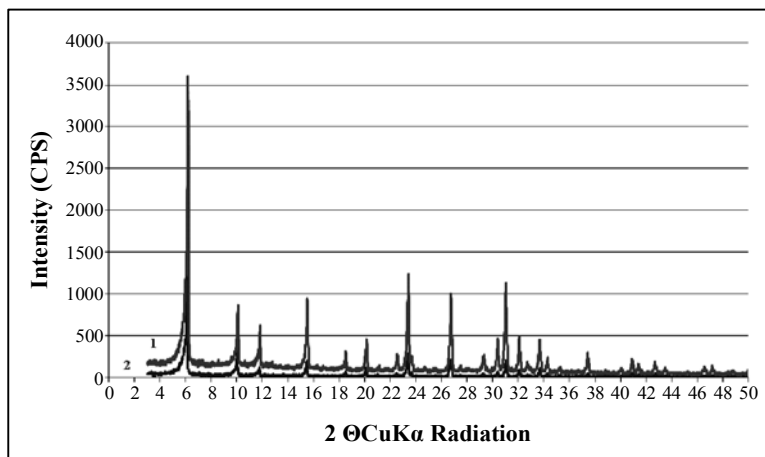


**Fig. 15: XRD diffractogram of modified synthetic Faujasite-13X (1) compared to raw synthetic Faujasite (2)**

The sorption of cationic surfactant on zeolite surfaces will result insignificant changes to rigid cage structure, and the XRD spectra of SMZ and natural Clinoptilolite was identical. This is also explained the results obtained from the natural (Jordanian and Syrian zeolite) and synthetic Faujasite-13X, which remain identical spectra to SMZ. In these results, the peaks intensity exhibit a significant changes; this increase in minerals content can be refer to its separation from other minerals in zeolitic tuff<sup>26</sup>.

### Chemical composition

Surfactant-modified zeolite samples were analyzed by XRF technique to identify the chemical composition changes due to modification processes. The results of analysis are shown in Table 8.

**Table 8: Chemical composition surfactant-modified and raw zeolites**

Major oxides %	Jordanian-Faujasite (SMZ)	Raw	Clinoptilolite-rich tuff	Raw	Syrian-Zeolite	Raw	Synthetic Faujasite-13X	Raw
	SiO <sub>2</sub>	39.9	38.9	66.4	66.8	35.2	37.5	34.3
TiO <sub>2</sub>	0.80	0.91	0.24	0.82	1.38	1.63	0.01	0.03
Al <sub>2</sub> O <sub>3</sub>	13.7	13.2	11.9	12.10	9.44	10.3	23.9	24.5
Fe <sub>2</sub> O <sub>3</sub>	4.82	5.62	1.42	1.58	8.72	9.93	0.04	0.05

Cont...

Major oxides %	Jordanian-Faujasite (SMZ)	Raw	Clinoptilolite-rich tuff	Raw	Syrian-Zeolite	Raw	Synthetic Faujasite-13X	Raw
MnO	0.15	0.15	0.06	0.07	0.12	0.13	0.00	0.00
MgO	4.10	4.73	1.10	1.19	8.75	8.85	0.00	0.11
CaO	9.44	10.2	2.72	3.13	12.3	15.7	0.03	0.41
Na <sub>2</sub> O	2.17	2.31	0.64	0.68	2.12	2.58	13.2	14.5
K <sub>2</sub> O	1.95	1.90	2.90	3.01	1.03	1.15	0.01	0.00
P <sub>2</sub> O <sub>5</sub>	0.44	0.44	0.05	0.06	0.57	0.68	0.00	0.02
LOI	21.8	20.8	11.8	10.3	19.6	10.7	27.7	24.0
Total	99.3	99.5	99.23	99.7	99.23	99.0	99.19	98.0

Results from the table above, exhibit an increase in SiO<sub>2</sub> content for Jordanian-Faujasite and decreased for the other zeolite samples. L.O.I. also exhibits an increase due to samples modification which reflects the increase in the organic matter on the surface of the zeolitic tuff minerals. As a result of modification the decrease in the inorganic cations (Ca<sup>2+</sup>, Mg<sup>2+</sup>, Na<sup>+</sup>, and K<sup>+</sup>) refer to replacing the zeolite surface by cationic surfactant molecules, which is with an agreement with literature<sup>22</sup>. The modification of zeolite by cationic surfactant is occurred by replacing inorganic cations by surfactant molecules.

#### FTIR of pure cationic surfactant

The IR absorption spectrum of the HDTMA-Br was measured, peaks analysis obtained from the spectra are shown in Table 9.

**Table 9: Infrared absorption bands of HDTMA-Br**

HDTMA-Br	Assignment <sup>a</sup>
722.62 (W)	[CH <sub>2</sub> ] at 725 cm <sup>-1</sup>
1473.14 (s)	[CH <sub>2</sub> ] at 1465 cm <sup>-1</sup>
2849.16 (S)	V <sub>sy</sub> [CH <sub>2</sub> ] at 2853 cm <sup>-1</sup>
2917.74 (S)	V <sub>as</sub> [CH <sub>2</sub> ] at 2926 cm <sup>-1</sup>

a: Reference<sup>26</sup>

### FTIR interpretation of surfactant-modified zeolite

IR absorption spectra were measured on modified zeolites and the results are shown in Table 13. For modified zeolite the IR measurements were applied on both coverage of surfactant at 50% and 200% to evaluate the zeolite surface loading with surfactant.

To study the molecular conformation of HDTMA chains on natural and synthetic zeolite, the most intense absorption bands at 2918 and 2849  $\text{cm}^{-1}$  in the FTIR spectrum of the crystalline HDTMA-Br were associated with the antisymmetric ( $\nu_{\text{as}}\text{CH}_2$ ) and symmetric ( $\nu_{\text{sy}}\text{CH}_2$ ) C–H stretching vibration modes of the methylene groups, respectively<sup>27-29</sup>.

In the IR spectra of saturated alkanes, there are two distinct peaks observed for the methylene stretching modes (asymmetric,  $\nu_{\text{as}} [\text{CH}_2] = 2926 \text{ cm}^{-1}$ , and symmetric,  $\nu_{\text{sy}} [\text{CH}_2] = 2853 \text{ cm}^{-1}$ )<sup>30,31</sup>.

**Table 10: Infrared absorption bands of surfactant-modified zeolite samples**

Jordanian-Faujasite	Syrian Zeolite	Clinoptilolite-rich tuff	Synthetic Faujasite-13X	Assignment
443.07	443.64	456.81	464.24	[T-O] at 400-500 $\text{cm}^{-1}$
1020.98	1014.65	1065.79	1015.84	[Si-O-Si (Al) at 1000-1200 $\text{cm}^{-1}$
1649-3446	1645-3444	1644-3671	1636-3482	[H <sub>2</sub> O] at 1600-3700 $\text{cm}^{-1}$
2852	2847	2852	2852	$\nu_{\text{sy}} [\text{CH}_2]$ at 2853 $\text{cm}^{-1}$
2924	2925	2919	2924	$\nu_{\text{as}} [\text{CH}_2]$ at 2926 $\text{cm}^{-1}$

### Adsorption results

#### Effect of initial concentration on aniline and its derivatives uptake

To study the effect of initial concentration on aniline and its derivative uptake by SMZ, using initial concentrations of 5, 15, 25, 50, 100, and 200 mg/L. This experiment was carried out at the pH 4.63, 4.85, and 5.1 for aniline, N-Methylaniline, N,N-Dimethylaniline, respectively. Research showed that the 24 hr. was sufficient to attain sorption equilibrium for non ionic benzene derivatives, chlorinated aliphatic compounds, and inorganic anion<sup>32</sup> and was assumed sufficient for phenol and aniline sorption<sup>33,34</sup>.

The effect of initial aniline, N-Methylaniline, N,N-Dimethylaniline concentration on adsorption by natural and synthetic zeolite revealed that the maximum adsorption of aniline by surfactant modified zeolite was 50%, represented by clinoptilolite-rich tuff. The maximum adsorption of aniline by other zeolite is: 28.4%, 45.6%, and 20% for Jordanian-Faujasite, Syrian-zeolite, and synthetic Faujasite, respectively. Modification of zeolite in this work was up to 100% of ECEC and this is due to the repulsion of the anilinium cation from SMZ treated to bilayer coverage<sup>35</sup>.

The result of initial N-Methylaniline concentration uptake by SMZ is adsorption of N-Mehylaniline by SMZ is 69.5% represented by Syrian Zeolite; this is may be due to the high surface area of Syrian zeolite. Clinoptilolite-rich tuff, Jordanian-Faujasite, and synthetic Faujasite exhibit maximum adsorption of N-Methylaniline of 58%, 41%, and 28%, respectively. The results of initial N,N-Dimethylaniline concentration shows a lower adsorption uptake compared to the aniline and N-Methylaniline adsorption uptake, the maximum adsorption uptake by natural zeolite (SMZ). Initial N,N-Dimethylaniline concentration uptake by synthetic Faujasite is negligible.

Jordanian-Faujasite shows the highest adsorption of N, N-Dimethylaniline represented by 16%, followed by 12.5% and 13% for clinoptilolite-rich tuff and Syrian zeolite, respectively. The highest uptake of N,N-Dimethylaniline by Jordanian-Faujasite resulted as the presence of faujasite mineral which has the largest diameter  $7.4 \text{ \AA}$ <sup>36</sup>, this is refer to the large size of N,N-Dimethylaniline. A comparison chart column of the maximum adsorption of aniline and its derivative by SMZ is shown in Fig. 16.

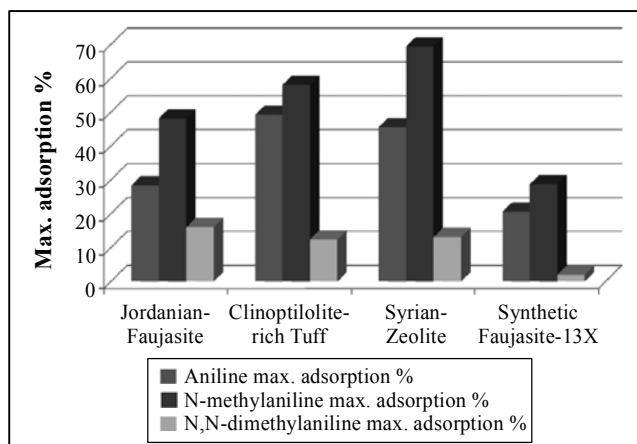


**Fig. 16: Comparison between organic pollutant maximum adsorption uptakes by different types of SMZ**

Linearized Freundlich adsorption isotherm was applied to analyze the data obtained from the adsorption experiments. Aniline and its derivative uptake by SMZ were fit to Freundlich adsorption isotherm and not applicable to Langmuir, this is due to the fact that the surface of adsorbent is heterogeneous and the adsorption followed a physical adsorption (i.e. van der Waals forces).

The results of linearized Freundlich adsorption isotherm of N-Methyl aniline uptake by modified Jordanian faugisite and synthetic zeolite are shown in Fig. 17 and N, N-Dimethylaniline experiments results are shown in Fig. 18.

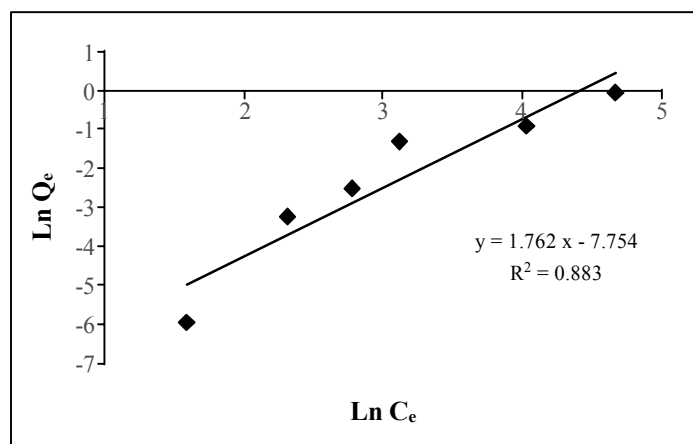


**Fig. 17: Linearized Freundlich adsorption isotherm of N-Methylaniline by modified Jordanian-Faujasite**

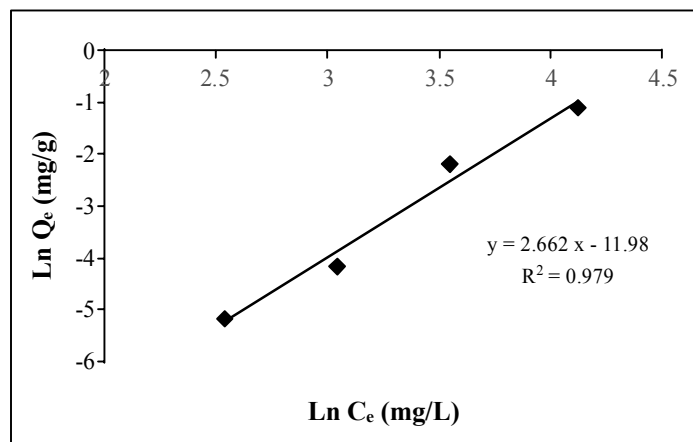


**Fig. 18: Linearized Freundlich adsorption isotherm of N-Methylaniline by modified synthetic Faujasite-13X**

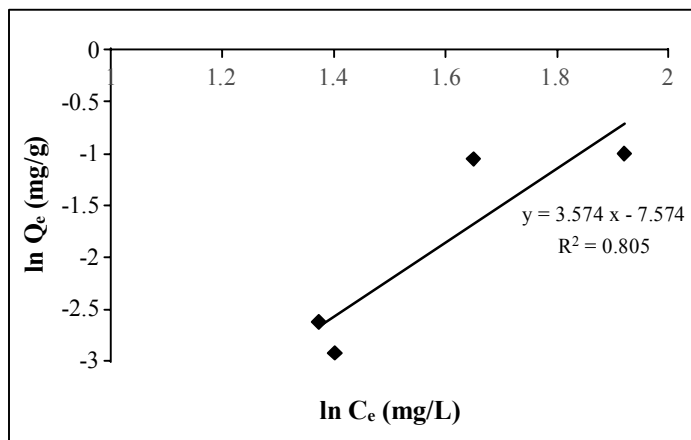


**Fig. 19: Linearized Freundlich adsorption isotherm of N,N-Dimethylaniline by modified Syrian zeolite**

The relationship between  $C_e$  vs.  $Q_e$  gives an indication of isotherm model classification shows the relationship between  $C_e$  vs.  $Q_e$  for aniline and its derivatives adsorption by the different types of SMZ.

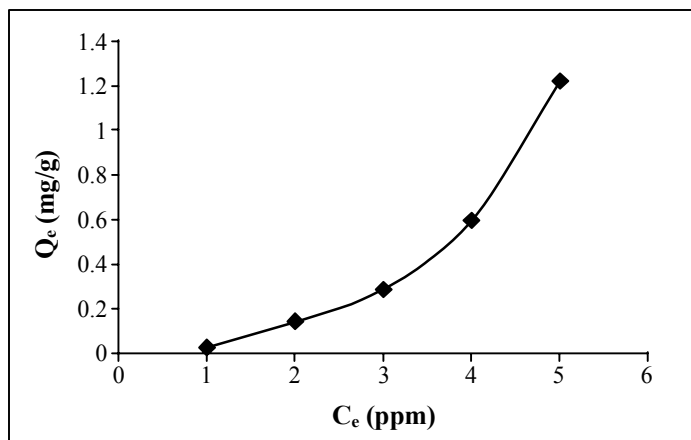


**Fig. 20:  $C_e$  vs.  $Q_e$  of aniline adsorption onto Syrian-natural zeolite**

The relationship between  $C_e$  vs.  $Q_e$  for aniline adsorptions indicate C-type isotherm, which reflect that the availability of sorbing sites is constant with increasing solute concentration due to the increase in the sorbent phase.

Same relationship between  $C_e$  vs.  $Q_e$  (C-type isotherm) goes for N-Methylaniline adsorption by SMZ.

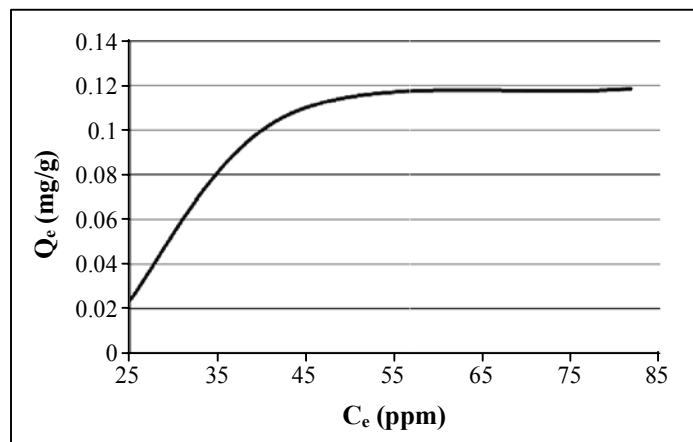


**Fig. 21:** C<sub>e</sub> vs. Q<sub>e</sub> of N, N-Dimethylaniline adsorption onto Jordanian-Faujasite

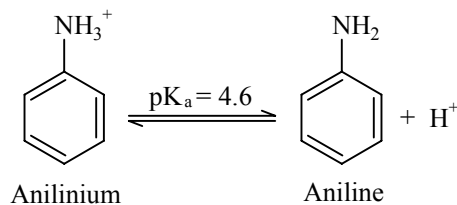
The relationship between C<sub>e</sub> vs. Q<sub>e</sub> for N,N-Dimethylaniline adsorption by SMZ represents L-type isotherm, which reflects high affinity between the adsorbate and adsorbent, and is usually indicative of chemisorptions.

### Effect of pH solution on adsorption of aniline and its derivatives

The pH of a solution is one of the most important parameters affecting the adsorption process. It is reported that pH of the solution would affect both aqueous chemistry and surface binding sites of the adsorbent. Moreover, a change in pH also results in a change in charge profile of adsorbate species, which consequently influences the interactions between the adsorbate species and adsorbent.

To study the effect of the solution pH on the adsorption of aniline and its derivative, batch test was carried out. Supernatants were analyzed by UV/Vis spectrophotometer.

Aniline exists in solution as protonated and deprotonated species, with the proportions being a function of pH<sup>35</sup>. Aniline is a weak base that can be protonate to form the anilinium ion as shown below.



**Schematic diagram shows the equilibrium state of aniline**

Aniline was repulsed by positive polarization in the acid solution because it was protonated by strong Bronsted acid and become anilinium cation, but was attracted because it was deprotonated by strong Bronsted base and become anilinium anion. On the other hand, the donored electron capability amino group increases in the basic solution<sup>36</sup>.

Since the aniline is pH dependent, sorption of aniline by SMZ should vary with pH<sup>37-40</sup>. It is concluded that the sorption efficiencies of aniline are high and stable under acidic and neutral pH conditions and decrease with the increase of pH value under alkaline pH conditions. Lower sorption of aniline at alkaline pH is probably due to the presence of excess OH<sup>-</sup> ions competing with aniline for hydrogen bond formed with water molecules.

Uptake of aniline by different types of SMZ shows different optimum pH. The efficiency of individual material at different pH ranges. Jordanian-Faujasite (Fig. 22) indicates that the maximum  $Q_e$  is 0.54 mg/g at pH 5 and decrease at lower and upper pH 5.

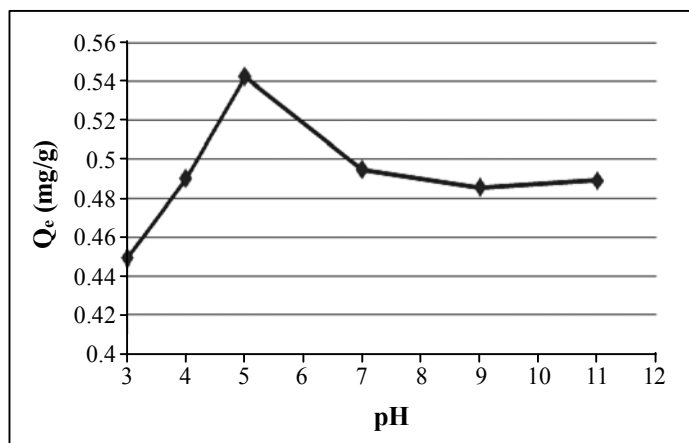


**Fig. 22: Effect of Jordanian-Faujasite pH on aniline removal**

In respect of clinoptilolite-rich tuff the relationship between pH and  $Q_e$  is reversible from pH 3 to 7, and then slightly increase from 7 to 11 as a result of converted aniline to anilinium cation as pH increase. The maximum  $Q_e$  value is about 0.85 mg/g. Syrian zeolite exhibit unclear trend at pH less than 7 and become clear trend at pH more than 7. The maximum  $Q_e$  value is 0.66 mg/g at pH 11.

For synthetic Faujasite-13X the maximum  $Q_e$  value is about 0.42 mg/g at pH 11, indicate that the  $Q_e$  is clear trend between pH 3-7 shows a zigzag trend and the trend become a proportional as pH more than 7. This may be this is due to adsorb anilinium cation into the



internal surface of surfactant modified-zeolite, which is still has a negative charge. As pH increase the aniline converted to anilinium ion.

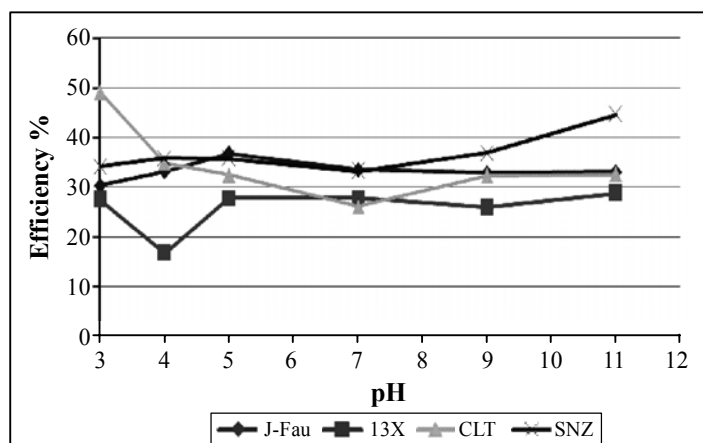


**Fig. 23: Comparison of different SMZ pH on aniline uptake**

This variation can be explained according to the pH experiment, the zeolite that show the low pH was clinoptilolite-rich tuff represented by maximum removal efficiency of aniline (49%) the highest pH was synthetic Faujasite-13X and indicated lower removal efficiency (28.8%). For Jordanian-Faujasite and Syrian-zeolite the efficiency removal was 36.8%, 44.6%, respectively. The optimum pH of aniline and its derivatives that effect on the adsorption process of the uptake by SMZ was examined under different pH. Fig. 24 shows the optimum pH values of aniline, N-Methylaniline, and N,N-Dimethylaniline of the adsorption uptake by different adsorbent.

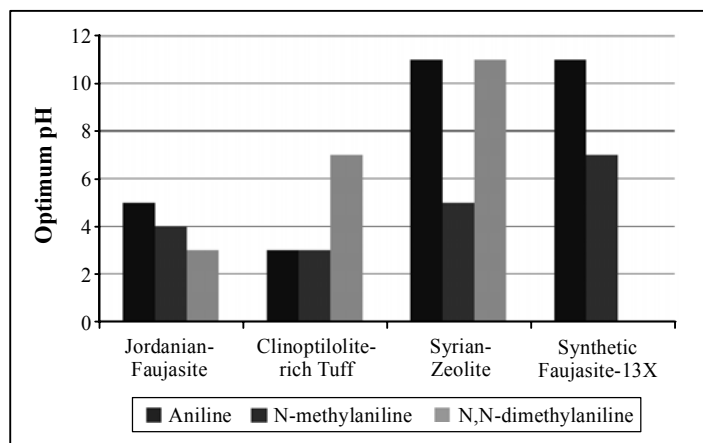


**Fig. 24: Optimum pH of aniline and its derivative of the uptake by SMZ**

## CONCLUSIONS

The characterization results show a variation of CEC ranges from 300 meq/100g, for synthetic zeolite, 158 meq/100 g for Jordanian-Faujasite, 142 meq/100 g) for Syrian-zeolitic, and for clinoptilolite-rich tuff was 93 meq/100 g. All types of zeolite show low specific gravity ranges from 2.12-2.33 g/m<sup>3</sup> and the pH experiments show that the zeolite acting as alkaline materials.

No changes occurred in minerals during the modification of zeolite except for Syrian zeolitic tuff, which exhibits an enhancement during modification led to identify zeolitic mineral (phillipsite) and clay mineral (Montmorillonite). Jordanian zeolitic tuff contains faujasite and phillipsite minerals, clinoptilolite-rich tuff only contain on clinoptilolite mineral. In respect of synthetic Faujasite-13X only faujasite mineral was recorded.

Chemical composition show a decrease in inorganic cation (Na<sup>+</sup>, K<sup>+</sup>, Mg<sup>2+</sup>, Ca<sup>2+</sup>) on the external surface of zeolite resulted as a modification by cationic surfactant molecules, also an increase of SiO<sub>2</sub> content occurred in all zeolite samples.

Scanning electron microscopy shows the geomorphology of the zeolite surface, varies between faujasite rim, prismatic and radial phillipsite, thin bladed clinoptilolite, to spheroidal cubic synthetic faujasite.

Adsorption of tested organic pollutants by surfactant modified zeolites was best fitted to Freundlich adsorption isotherm more than Langmuir; this is due to heterogeneity of the adsorbent surface.

Different types of adsorbent have been tested to remove aniline and its derivatives by adsorption technique and it was noticed that it is depend on the pollutants itself and on the adsorbent as well.

The removal efficiency of aniline was 50% by clinoptilolite-rich tuff, and 28.4%, 45.6%, and 20% for Jordanian-Faujasite, Syrian-zeolite, and synthetic Faujasite, respectively.

The removal efficiency of N-Methylaniline was 69.5% by Syrian-zeolite, and 58%, 48%, and 28% by Clinoptilolite-rich tuff, Jordanian-Faujasite, and synthetic Faujasite, respectively.

The removal efficiency of N, N-Dimethylaniline was 16% by Jordanian-Faujasite, and 13%, 12.5% by clinoptilolite-rich tuff and Syrian-zeolite respectively, and negligible for synthetic Faujasite-13X.

Since the data was best fitted to Freundlich adsorption isotherm (n) value for all natural adsorbent isotherms varies between 0.51-0.9 for aniline and N-Methylaniline adsorption represented the difficulty of adsorption, while for synthetic adsorbent the adsorption was favorable.

Adsorption of N, N-Dimethylaniline by Jordanian-Faujasite and clinoptilolite-rich tuff show a difficulty in adsorption (depending on n value), and while for Syrian-zeolite show a favorable adsorption.

The pH of a solution is one of the most important parameters affecting the adsorption process, aniline, N-Methylaniline, and N, N-Dimethylaniline has a certain pKa value (4.63, 4.85, and 5.1 respectively) that affect on its equilibrium state.

The sorption efficiencies of aniline and its derivatives are high and stable under acidic and neutral pH conditions.

### **ACKNOWLEDGEMENT**

Authors would like to thank the colleagues in the Chemistry Department in the Hashemite University for help and support in analytical and interpretation of the results.

### **REFERENCES**

1. S. M. Rustamov, Z. Z. Bashirova, F. M. Nasiri, A. I. Yagubov and S. A. Muradova, Use of Natural Zeolites for Purification of Industrial Wastewater from Toxic Organic Chlorine Compounds (1988). In D. Kallo, H. S. Sherry (Editors), 2<sup>nd</sup> International Conference on the Occurrence, Properties and Utilization of Natural Zeolites, Budapest, Hungary, August 12-16 (1985).
2. R. S. Bowman, Applications of Surfactant-Modified Zeolites to Environmental Remediation, Microporous Mesoporous Materials (2002), 7<sup>th</sup> International Conference on the Occurrence, Properties, and Utilization of Natural Zeolites, Socorro, New Mexico, USA, July 16-21 (2006).
3. V. Jovanovic, V. Dondur, Li. Damjanovic, J. Zakrzewska and M. Tomasevic-Canovic, Improved Materials for Environmental Application: Surfactant-Modified Zeolites, Materials Science Forum, **518**, 223-228 (2006).
4. D. W. Breck, Zeolite Molecular Sieves, John Wiley, New York, USA (1974) p. 771.
5. D. Krantz and B. Kifferstein, Water Pollution and Society, [www.umich.edu / society / waterpollution.htm](http://www.umich.edu/society/waterpollution.htm) (2006).

6. Mediterranean Environmental Technical Assistance Program/Water Quality Management/Jordan [Online] Available: <http://Inweb18.worldbank.org/mna/mena.nsf/Attachement/WQM+Jordan+Profile+A4/File/WQM+Jordan+A4.pdf>.
7. Jordan, Water availability and Demand, [www.kinghussein.gov.jo/env4.html](http://www.kinghussein.gov.jo/env4.html).
8. [http://66.102.9.104/search?q=cache:0C1\\_57\\_f8iMJ:Inweb18.worldbank.org/mna/mena.nsf/Attachements/WQM%2BJordan%2BProfile%2BA4%24FileWQM%2BJordan%2BA4.pdf+Jordan,+Water+Availability+and+Demand&hl=en&ie=UTF-8](http://66.102.9.104/search?q=cache:0C1_57_f8iMJ:Inweb18.worldbank.org/mna/mena.nsf/Attachements/WQM%2BJordan%2BProfile%2BA4%24FileWQM%2BJordan%2BA4.pdf+Jordan,+Water+Availability+and+Demand&hl=en&ie=UTF-8).
9. C. J. Schollenberger and R. H. Simon, Determination of Exchange Capacity and Exchangeable Bases in Soil-Ammonium Acetate Method, *J. Soil Sci.*, **59**, 13-24 (1945).
10. Z. Li, T. Burt and R. S. Bowman, Sorption of Ionizable Organic Solutes by Surfactant-Modified Zeolite, *Environ. Sci. Technol.*, **43**, 3756-3760 (2000).
11. K. M. Ibrahim, Geology, Mineralogy, Chemistry, Origin and Uses of the Zeolites Associated with Quaternary Tuffs of North East Jordan, Ph.D. Thesis, Royal Holloway, University of London, U.K. (1996) p.254.
12. I. M. Dwairi, A Chemical Study of the Palagonitic Tuff of the Aritain Area of Jordan, With Special Reference to Nature, Origin and Industrial Potential of the Associated Zeolite Deposits, Ph.D. Thesis, Hull University, UK (1987).
13. G. Gottardi, Mineralogy and Crystal Chemistry of Zeolites, in: L. B. Sand and F. A. Mumpton (Editors) *Natural Zeolites, Occurrence, Properties, and Use*, Pergamon Press, Oxford (1978) pp. 31-44.
14. D. W. Ming and F. A. Mumpton, Zeolites in Soils. In: Dixon, J. B. and Weed, T. B. (Editors), *Minerals in Soil Environment*, 2<sup>nd</sup> Editions, Soil Science Society, U.S.A. (1989).
15. E. M. Flanigen, Crystal Structure and Chemistry of Natural Zeolites. In: F. A. Mumpton (Editor) *Mineralogy and Geology of Natural Zeolites*, Review in Mineralogy, *Mineral. Soc. Am.*, **Vol. 4**, pp. 19-51 (1981).
16. G. Cruciani, Zeolites Upon Heating: Factors Governing their Thermal Stability and Structural Changes, *J. Phys. Chem. of Solids*, **67(9-10)**, 1973-1994 (2006).
17. T. I. Avdeeva, I. A. Vorsina and A. A. Novolodskaya, Infrared Spectra of Potassium and Sodium Aluminosilicates Hydrates, *Sib. Chem. J. Academic Sci., USSR, Novosibirsk*, 671 (1969).

18. E. M. Flanigen, H. Khatmami and H. A. Szymanski, Infrared Structural Studies of Zeolite Frameworks, in, *Molecular Sieve Zeolite-I*, Adv. Chem. Ser., (R. F. Gould, Ed.), Am. Chem. Soc., Washington, D.C (1971) pp. 201-229.
19. I. A. Belitskii and G. A. Golubova, Infrared Spectra of Natural Zeolites, *Mater. Genet. Eksp. Mineral*, **7** (1972) p. 310 (in Russian).
20. I. Vergilov, L. Filizova and G. N. Kirov, Infrared Spectroscopic Study of Zeolites from the Heulandite Group of Minerals, *Izv. Geol. Inst., Bulg. Akad. Nauk., Ser. Geokhim., Mineral, Petrogr.* (Bulgarian) **22** (1973) p. 81.
21. G. E. Christidis, D. Moraetis, E. Keheyanyan, L. Akhalbedashvili, N. Kekelidze, R. Gevorkyan, H. Yeritsyan and H. Sargsyan, Chemical and Thermal Modification of Natural HEU-type Zeolitic Materials from Armenia, Georgia and Greece, *J. Appl. Clay Sci.*, **24(1-2)**, 79-91 (2003).
22. M. Majdan, M. Kowalska-Ternes, S. Pikus, P. Staszczuk, H. Skrzypek and E. Zieba, Vibrational and Scanning Electron Microscopy Study of the Mordenite Modified by Mn, Co, Ni, Cu, Zn and Cd, *J. Molecular Structure*, **649(3)**, 279-285 (2003).
23. S. C. Boufard and S. J. B. Duff, Uptake of Dehydroabietic Acid using Organically-Tailored Zeolites, *Water Research*, **34**, 2469-2476 (2000).
24. J. A. Smith and A. Galan, Sorption of Nonionic Organic Contaminants to Single and Dual Organic Cation Bentonites from Water, *Environ. Science Technology*, **29(3)**, 685-692 (1995).
25. R. Leyva-Ramos, A. Jacobo-Azuara, P. E. Diaz-Flores, R. M. Guerrero-Coronado, J. Mendoza-Barron and M. S. Berber-Mendoza, Adsorption of Chromium (VI) from an Aqueous Solution on a Surfactant-Modified Zeolite, *Colloids and Surfaces A: Physicochemical and Engineering Aspects*, **330(1)**, 35-41 (2008).
26. J. S. Janks and F. Cadena, Identification and Properties of Modified Zeolites for the Removal of Benzene, Toluene, and Xylenes from Aqueous Solutions, Presented at the 66<sup>th</sup> Annual and Technical Conference and Exhibition of the Society of Petroleum Engineers, in Dallas, TX, USA, 153-167 (1991).
27. H. Lee, Y. S. Park, T. S. Kim, Y. Lee and K. B. Yoon, Separation of Mixtures of Zeolites and Amorphous Materials and Mixtures of Zeolites with Different Pore Sizes into Pure Phases with the Aid of Cationic Surfactants, *Chemistry of Materials*, **14(8)**, 3260-3270 (2002).
28. B. S. Furniss, A. J. Hannaford, V. Rogers, P. G. Smith and A. R. Tatchell, *Vogel's Textbook of Practical Organic Chemistry*, Longman Group Limited, London (1978).

29. H. Hongping, F. L. Ray and Z. Jianxi, Infrared Study of HDTMA<sup>+</sup> Intercalated Montmorillonite, *J. Spectrochimica Acta Part A: Molecular and Biomolecular Spectroscopy*, **60(12)**, 2853-2859 (2004).
30. X. Yu, L. Zhao, X. Gao, X. Zhang and N. Wu, The Intercalation of Cetyltrimethylammonium Cations into Muscovite by a Two-Step Process: II, The Intercalation of Cetyltrimethylammonium Cations into Li-muscovite, *J. Solid State Chem.*, **179(5)**, 2853-2859 (2006).
31. J. M. Mellott, W. A. Hayes and D. K. Schwartz, Kinetics of Octadecyltrimethyl ammonium Bromide Self-Assembled Monolayer Growth at Mica from an Aqueous Solution, *Langmuir* (2004) pp. 2342-2348.
32. W. A. Hayes and D. K. Schwartz, Two-Stage Growth of Octadecyltrimethyl ammonium Bromide Monolayer at Mica from Aqueous Solution Below the Kraft Point, *Langmuir*, **14** (1988) pp. 5913-5917.
33. Z. Li and R. S. Bowman, Counterion Effects on the Sorption of Cationic Surfactant and Chromate on Natural Clinoptilolite, *Environ. Sci. Technol.*, **31**, 2407-2412 (1997).
34. R. S. Bowman, G. M. Haggerty, R. G. Huddleston, D. Neel, M. M. Flynn, in, *Surfactant-Enhanced Subsurface Remediation*, D. A. Sabatini, R. C. Knox, J. H. Harwell (Eds.), ACS Symposium Series 594, American Chemical Society, Washington, DC (1995) pp. 54-64.
35. G. M. Haggerty and R. S. Bowman, Sorption of Chromate and Other Inorganic Anions by Organo-Zeolite, *Environ. Sci. Technol.*, **28**, 452-458 (1994).
36. R. S. Bowman, E. J. Sullivan and Z. Li, Uptake of Cations, Anions, and Nonpolar Organic Molecules by Surfactant-Modified Clinoptilolite-Rich Tuff, In *Natural Zeolites for the Third Millennium*, C. Colella and F. A. Mumpton (Eds.), Napoli, Italy, De Frede (Editor) (2000) pp. 287-297.
37. <http://radiantlyalive.com/What%20is%20zeolite.pdf>.
38. Y. Hu, G. J. Liu and H. H. Xu, *Adsorption Action* 1<sup>st</sup> Edition, Shanghai Technology Literature Publishing Company (Chinese) (1989).
39. A. Ornek, M. Ozacar and I. A. S. Iengil, Adsorption of Lead onto Formaldehyde or Sulphuric Acid Treated Acorn Waste, Equilibrium and Kinetic Studies, *Biochem. Eng. J.* **37**, 192-200 (2007).

40. Y. Han, X. Quan, S. Chen, H. Zhao, C. Cui and Y. Zhao, Electrochemically Enhanced Adsorption of Aniline on Activated Carbon Fibers, Separation and Purification Technol. J., **50(3)**, 365-372 (2006).

*Revised : 26.05.2014*

*Accepted : 29.05.2014*